Engineering Structures 195 (2019) 400–412

Contents lists available at ScienceDirect

Engineering Structures

journal homepage: www.elsevier.com/locate/engstruct

A procedure to design toe protections for rockfill dams against extreme through-flows

Rafael Morán[a,b,*], Miguel Á. Toledo[a], Antonia Larese[c,b], Ricardo Monteiro-Alves[a]

[a] Dept. of Civil Engineering: Hydraulics, Energy and Environment, Universidad Politécnica de Madrid, E.T.S. de Ingenieros de Caminos, Canales y Puertos, C/ Profesor Aranguren, 28040 Madrid, Spain

[b] International Centre for Numerical Methods in Engineering, Universitat Politècnica de Catalunya, Campus Nord, C/ Gran Capita, 08034 Barcelona, Spain

[c] Università degli Studi di Padova. Department of Mathematics "Tullio Levi Civita", Torre Archimede, via Trieste 63, 35131 Padova, Italy

ABSTRACT

This article presents a procedure for designing rockfill toe protections with a highly permeable downstream shoulder to avoid mass sliding in dams during extremely high through-flow episodes. This accidental through-flow may be caused by reasons such as overtopping or leakage flow due to the loss of sealing at the impervious element of the dam or its foundation. The proposed protection is located at the downstream toe of the dam, and it is composed of highly permeable material, typically compacted rockfill. This material can be different from the rockfill forming the downstream shoulder of the main dam. The work is a result of a combination of numerical and experimental research carried out to analyze the influence of the geometry of the toe protection for given material properties of both dam shoulder and protection, when they can be considered highly isotropic. As a result of these studies, a design methodology is obtained. A series of validation tests are presented to support the reliability of the method.

Symbols with the subscripts *E* and *Eb* refer, respectively, to the rockfill material of the dam shoulder and to the material of the toe protection.

1. Introduction and background

During the last decades, the social demand for dam safety standards has significantly increased, especially in most developed countries. This has yielded new and more demanding dam regulations and technical guidelines, some of them imposing the need of protecting existing dams [1,2]. The dam protection techniques involve different adaptations of the designs of the dams to protect them against foreseeable failure mechanisms so as to improve their safety [3,4].

There are different types of dam protections, mainly depending on the type of dam, the associated failure mechanisms, and the specified degree of protection [5]. In the particular case of rockfill or earthfill dams, the development of heavy through-flows within the downstream shoulder due to overtopping or extremely high leakages (Fig. 1) is the main cause of their partial or total failure [6]. Reinforced rockfill, riprap, and gabions, among others, have been the most common rockfill dam protections used in the past [7–11].

In addition to this, countries such as Norway or Sweden are currently using rockfill protections on the downstream slope in rockfill dams where potential risk for loss of life and significant downstream damage is high. This is the case of, for example, *Suorva, Seitevare* and *Trängslet Dams* in Sweden, and *Svartevann Dam* in Norway. So-called "rockfill toe berms" are installed on these three Swedish dams, whereas rip-rap is placed on the downstream slope of the Norwegian dam. These particular types of protection have been recommended by their respective National Dam Safety Guidelines [2,12] to improve the stability of dams against accidental leakage [13–16].

Likewise, thorough research on the mass instability caused by through-flow due to overtopping in rockfill dams has been developed during last decades [17–19] and there have been new, experimentally verified developments on the coupled problem of nonlinear seepage through-flow and mass-slide failure of rockfill dams [20–22]. Such research effort has made possible to develop an understanding of the failure mechanisms in rockfill dams as well as validate such numerical codes. As a result of this, it was concluded that the stability of the downstream shoulder plays a key role to avoid severe damages in the dam or its total failure [5,23–25]. Thus, when through-flow occurs, the downstream shoulder can be rapidly removed, and the impervious

* Corresponding author at: Dept. of Civil Engineering: Hydraulics, Energy and Environment, Universidad Politécnica de Madrid, E.T.S. de Ingenieros de Caminos, Canales y Puertos, C/ Profesor Aranguren, 28040 Madrid, Spain.

E-mail addresses: r.moran@upm.es (R. Morán), miguelangel.toledo@upm.es (M.Á. Toledo), antonia.larese@unipd.it (A. Larese), ricardo.monteiro@upm.es (R. Monteiro-Alves).

URLs: https://orcid.org/0000-0002-0031-1605 (R. Morán), https://orcid.org/0000-0002-7594-7624 (M.Á. Toledo), https://orcid.org/0000-0002-7284-3926 (A. Larese), https://orcid.org/0000-0002-2059-1712 (R. Monteiro-Alves).

https://doi.org/10.1016/j.engstruct.2019.06.004
Received 12 September 2018; Received in revised form 29 May 2019; Accepted 4 June 2019
Available online 11 June 2019

Nomenclature

a_i	coefficient of the first-order term of the parabolic equation of the seepage flow
b_i	coefficient of the second-order term of the parabolic equation of the seepage flow
A	relation between H_b and z_d
B	width of the crest of the toe protection
B_c	maximum advance of the damage caused by mass sliding
C_u	uniformity coefficient of the granular material
D_j	diameter at which j% of the gravel is comprised of stones with a diameter less than this value
i	hydraulic gradient
i_{max}	maximum hydraulic gradient at the downstream slope of the rockfill
F	stability safety factor for saturated rockfill slopes
H	dam height
H_b	toe protection height
H_b^*	toe protection height used in the experimental validation
K_j	inverse of the linear permeability of the material j for the maximum hydraulic gradient
K_{de}	equivalent linear permeability
K_{dj}	linear permeability of the material j for the maximum hydraulic gradient
K_j	inverse of the linear permeability of the material j
L	horizontal distance between the toe and the downstream end of the crest of the dam shoulder
L_P	horizontal distance between the downstream toe of the protection and point P
M1, *M2* and *M3*	designation of the three materials of the validation tests
n	porosity
N	rockfill slope of the downstream shoulder of the dam (H:V)
N_b	rockfill slope of the toe (H:V)
P	intersection point between the berm of the toe and the slope of the downstream shoulder of the dam
q_d	design unit discharge of the through-flow
q_s	unit discharge of the through-flow
q_r	unit discharge of the through-flow which causes the failure of the downstream shoulder of the dam
v	bulk velocity
v_{max}	bulk velocity for the i_{max} hydraulic gradient
z_d	height of the saturation line at the slope of the existing dam
z_{db}	height of the saturation line at the contact surface between the downstream shoulder of the dam and the rockfill protection
α	angle between horizontal and the rockfill slope
β	pore pressure coefficient used in the stability equation of the saturated rockfill
$\gamma_{j,sat}$	saturated specific weight of the material j
γ_w	specific weight of the water
φ_j	internal friction angle of the material j

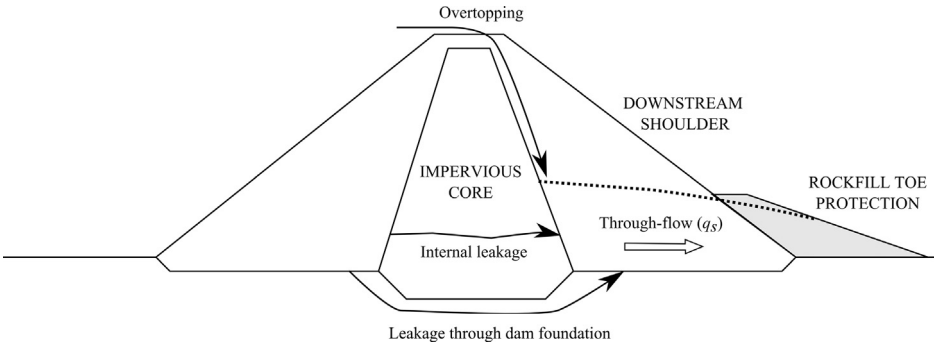

Fig. 1. Scheme of a rockfill toe protection for an existing dam ().
adapted from [5]

element would lose support. In such case, the dam could suddenly be breached. Therefore, the construction of a rockfill downstream toe, conducted to assure the stability of the downstream shoulder, would increase significantly the safety of the existing dam.

The aim of the article is to present a design procedure of rockfill toe protections in order to stabilize the downstream shoulder of the dam in extremely high through-flow conditions, where unexpected pore water pressures can develop within the rockfill material [26].

2. Design procedure

2.1. Overview

The procedure is applicable to existing rockfill dams with the downstream shoulder constructed on rock foundations (Fig. 1). Thus, the permeability of the foundation has been neglected, assuming that the through-flow seepage is developed through the downstream shoulder. Thereby, under high through-flow scenarios, the turbulent seepage flow is an external input that has to be estimated beforehand. Such estimation of the potential discharge per unit length of the toe berm (q_s) can be done considering extreme hydrologic episodes, the failure of the spillway or potential leakage flows due to a failure in the impervious element of the dam, among others. The protection is designed to resist through-flows within the downstream shoulder of the dam from inside to outside. However, its behavior under external skimming flow, parallel to the downstream slope of the existing dam, would not be acceptable given that the added material at the toe of the dam would perform as an obstacle to such flow, which may initiate erosive processes. This condition must be considered when estimating the height of the protection as will be shown later on. Moreover, the different materials are considered as an isotropic continuum. This means that this procedure is particularly applicable to dams with a not significantly layered rockfill material at the downstream shoulder. Such layering processes are especially relevant in weak rockfills due to the effect of the compaction energy of the heavy machinery and may cause a high variation of the permeability along the vertical direction.

In addition to q_s, other input parameters for the design procedure (Fig. 2) are the downstream slope of the dam (N), the internal friction angle (φ_E) and the saturated specific weight ($\gamma_{E,sat}$) of the rockfill material of the downstream shoulder (E). It is widely known [27,28] that

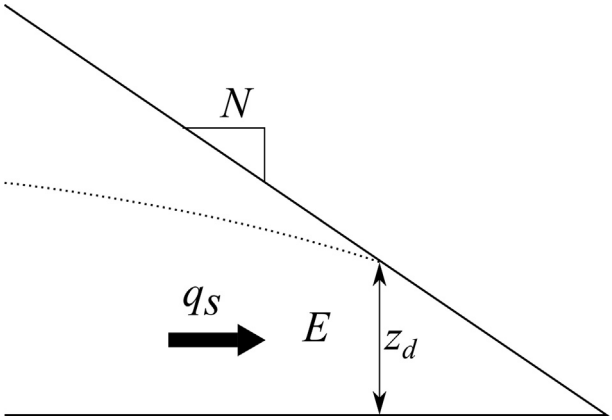

Fig. 2. Scheme of the saturation line of the seepage through-flow (q_s) at the toe of the downstream shoulder [5,26].

seepage flow through highly permeable continuum media implies a parabolic relation (Eq. (1)) between the hydraulic gradient (i) and the average seepage velocity in the continuum (v). Therefore, in this case, the permeability of the downstream rockfill material is not linear and has to be characterized by the coefficients a_E and b_E of (Eq. (1)).

$$i = a_E \cdot v + b_E \cdot v^2 \tag{1}$$

The output parameters of the design procedure (Fig. 3) are the width of the crest (B); the downstream slope (N_b); and the height (H_b) of the rockfill toe. The procedure assumes that the properties of the material of the rockfill toe (E_b) and the downstream shoulder (E) are known. The properties of both materials are stated by parameters with the sub-index E (dam) and E_b (protection).

Previous work by the authors concluded the design criteria for the crest width (B) and the slope of the rockfill protection (N_b) to remain stable in saturated conditions [29]. In such work, the authors stated that, for a given through-flow, the width of the crest (B) not only had a minor positive effect on the mass-slide stability of the dam and protection but also might generate a rise of the saturation line which could be harmful for the stability of the dam. These conclusions were based on a combination of experimental and numerical research. Therefore, the crest width should be chosen according to construction requirements, i.e., the minimum width needed for an appropriate compaction of the rockfill.

Additionally, Toledo obtained an expression (Eq. (2)) to obtain the mass-slide safety factor of the rockfill slope in saturated conditions [17].

$$F = \frac{1}{\gamma_{Eb,sat}} \cdot \left(\gamma_{Eb,sat} - \frac{\beta \cdot \gamma_w}{\cos^2 \alpha} \right) \cdot \frac{\tan \varphi_{Eb}}{\tan \alpha} \tag{2}$$

where:

F, safety factor
β, coefficient given by:

$$\beta = -0.32 \cdot N_b + 1.52 \cdot N_b - 0.77, \text{ if}(1.5 < Nb < 2) \tag{3}$$

$$\beta = 1, \text{ if}(Nb \geq 2) \tag{4}$$

N_b, rockfill slope (Horizontal:Vertical)
$\gamma_{Eb,sat}$, saturated specific weight of the material E_b
γ_w, specific weight of the water
φ_{Eb}, internal friction angle of the material E_b
α, angle between the horizontal and the rockfill slope, where,

$$\tan \alpha = 1/N_b \tag{5}$$

Consequently, applying (Eq. (2)) for a given safety factor (F), the stable slope could be obtained through the value of the angle (α). This angle directly determines the slope (N_b). Given that, in most of the cases, the friction angle of the rockfill materials results in a stable slope when N_b is higher than two, the coefficient β can be considered equal to one. This condition involves considering hydrostatic pore water pressure in the granular material, and, therefore, the obtained result is slightly conservative. Nevertheless, if the value N_b of the obtained slope is less than two, an iterative process could be done to consider a more accurate value of the coefficient β.

Given that this formulation (Eq. (2)) was obtained numerically, a set of validation tests was developed to verify its applicability for design purposes. This validation was made for slopes greater than two, i.e., for a value of coefficient β equal to one, obtaining successful results [26].

2.2. Estimation of the height of the rockfill toe protection

Once the width of the rockfill crest (B) and the stable slope (N_b) have been estimated according to construction requirements and (Eq. (2)), respectively, the last parameter to define the rockfill protection is the protection height (H_b).

The protection height has to be high enough to avoid the development of pore water pressures in the area of the downstream shoulder of the dam which is not covered by the material of the rockfill toe. Otherwise, the slope of the dam would not be stable since it is usually designed in dry conditions, i.e., in the absence of pore water pressures. Such condition implies that the height of the saturation line at the contact surface between the downstream shoulder of the dam and the rockfill protection (z_{db}) should not exceed H_b (Fig. 3) for a given through-flow (Eq. (6)).

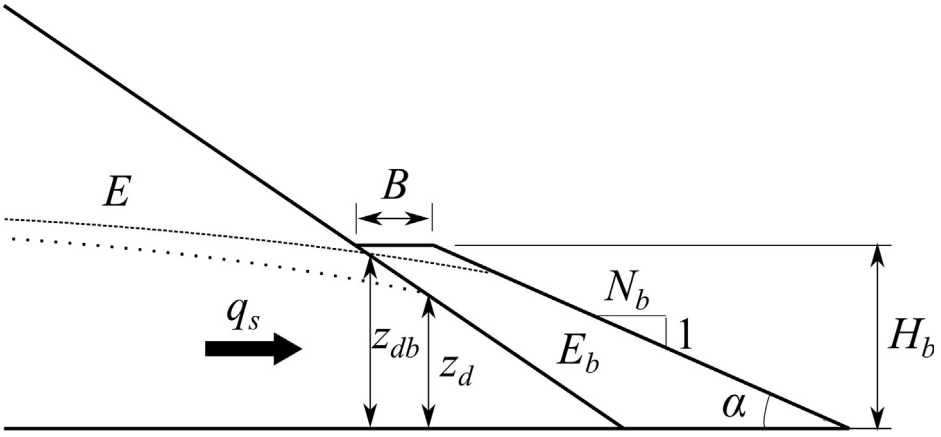

Fig. 3. Design parameters of a rockfill toe protection [5,26].

$$z_{db} \leq H_b \tag{6}$$

To do so, for a particular design through-flow (q_s), the height of the saturation line at the slope of the existing dam (z_d) has been considered as an additional input of the design methodology (Fig. 1). In such a way, z_d establishes a minimum value of H_b which could be finally calculated by an iterative process until the condition (Eq. (6)) is fulfilled. The value of z_d can be calculated by different numerical methods, such as the open source *Kratos* [http://www.cimne.com/kratos/] [30] which uses a finite element level set technique to trace the evolution of the transient seepage in variable porosity media, which assume the parabolic seepage equation using the Ergun approach [31,32].

At this point, the authors have deduced a formulation to a first estimation of H_b in order to complete the design procedure of the rockfill protection. The algorithm makes some conservative assumptions and simplifications which can be acceptable for design purposes, as it has been experimentally validated through a set of laboratory tests. Nevertheless, once H_b has been obtained according to this estimation, the development of a numerical seepage model of the proposed design is suggested as the final step of the design procedure.

The formulation to estimate H_b follows the basis of the research made by Toledo. In such research, it was stated that the hydraulic gradient at the toe of the rockfill has a maximum value (i_{max}) as a function of its downstream slope (N), expressed in (Eq. (7)) [23].

$$i_{max} = \frac{1}{N} \tag{7}$$

Assuming the conservative hypothesis that the hydraulic gradient is maximum, and constant, at the toe of the rockfill, it is possible to apply a linear seepage equation (Darcy's law), as a simplification for design purposes. Thus, a linear relationship between the maximum hydraulic gradient (i_{max}) and the maximum seepage velocity (v_{max}) can be obtained, expressed by the coefficient K_E or the linear permeability K_{dE} (Eq. (8)). In the same way, for K_{Eb} (Eq. (9)).

$$K_E = \frac{1}{K_{dE}} = \frac{i_{max}}{v_{max}} = \frac{1/N}{\frac{-a_E + \sqrt{a_E^2 + 4\cdot\frac{b_E}{N}}}{2\cdot b_E}} = \frac{2\cdot b_E}{N\cdot\left(-a_E + \sqrt{a_E^2 + 4\cdot\frac{b_E}{N}}\right)} \tag{8}$$

$$K_{Eb} = \frac{1}{K_{dEb}} = \frac{i_{max}}{v_{max}} = \frac{1/N_b}{\frac{-a_{Eb} + \sqrt{a_{Eb}^2 + 4\cdot\frac{b_{Eb}}{N_b}}}{2\cdot b_{Eb}}} = \frac{2\cdot b_{Eb}}{N_b\cdot\left(-a_{Eb} + \sqrt{a_{Eb}^2 + 4\cdot\frac{b_{Eb}}{N_b}}\right)} \tag{9}$$

Meanwhile, H_b can be expressed as a function of z_d (Eq. (10)):

$$H_b = A\cdot z_d \tag{10}$$

where

A is a coefficient greater than or equal to 1.

Therefore, H_b could be obtained through the estimation of the coefficient A. Obviously, this coefficient must meet the condition expressed in (Eq. (6)) for the particular crest width (B) and rockfill toe slope (N_b) which were fixed previously based on construction requirements and (Eq. (2)).

The minimum value of H_b would be precisely z_{db} (Eq. (11)), given that this would fulfill strictly the condition to avoid the development of pore water pressures in the surface of the downstream shoulder of the dam which is not secured by the protection material. In this case, the estimation of the coefficient A can be done through a theoretical approach assuming an equivalent linear permeability (K_{de}) in the medium defined by the rockfill protection and the toe of the covered part of the downstream shoulder (see the shaded area in Fig. 4) and making H_b equal to z_{db} (Eq. (11)).

$$H_b = z_{db} \tag{11}$$

Consequently, an equivalent permeability was theoretically deduced. As is known [33], when the seepage through a series of j materials disposed consecutively with permeability K_{dj} and thickness L_j, in which a total hydraulic head loss (Δh) occurs, the seepage flow (Q) keeps constant within a seepage tube (Fig. 5).

In such a case, the seepage flow can be expressed in terms of K_{de}:

$$v = K_{de}\cdot i_e \tag{12}$$

where

$$i_e = \frac{\Delta h}{\sum L_j} = \frac{\sum \Delta h_j}{\sum L_j} \tag{13}$$

and

$$\Delta h_j = \frac{L_j\cdot v}{K_j} \tag{14}$$

Then, substituting (Eq. (13)) and (Eq. (14)) in (Eq. (12)):

$$K_{de} = \frac{v}{i_e} = \frac{v}{\frac{\sum \Delta h_j}{\sum L_j}} = \frac{v}{\frac{\sum \frac{L_j\cdot v}{K_{dj}}}{\sum L_j}} = \frac{\sum L_j}{\sum \frac{L_j}{K_{dj}}} \tag{15}$$

Applying (Eq. (15)) to the seepage domain defined in Fig. 4 and admitting the assumption, for design purposes, that the length of the seepage path is L_E across the material (E) and L_{Eb} in the material of the rockfill protection (E_b), the equivalent permeability can be obtained (Eq. (16)):

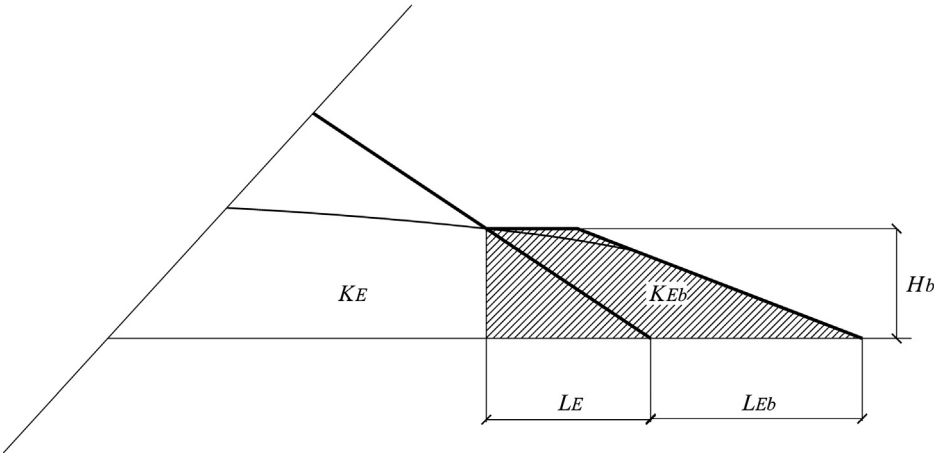

Fig. 4. Seepage area (shaded) with the imposed condition (Eq. (11)) [26].

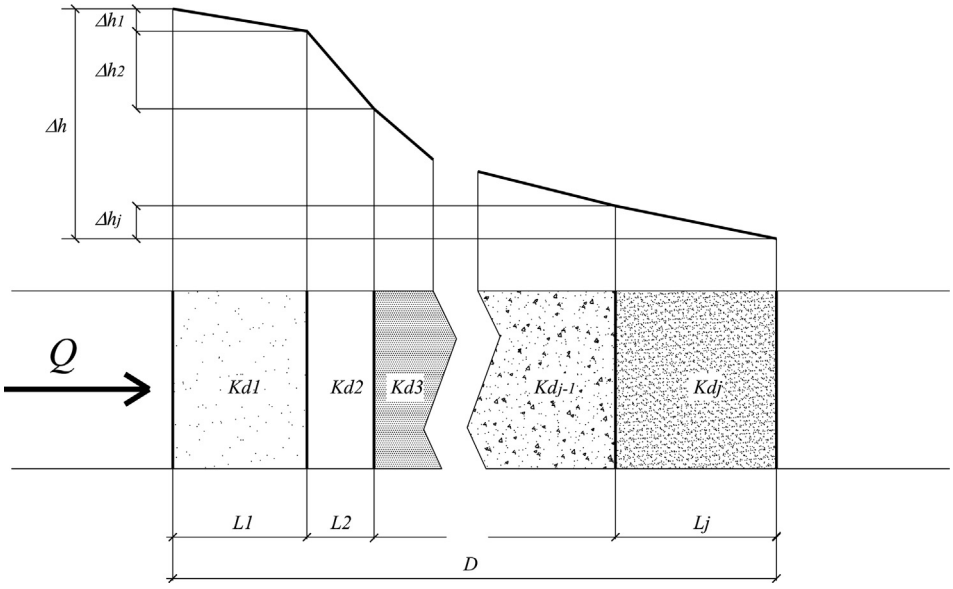

Fig. 5. One-dimensional scheme of the head losses of the seepage flow (Q) through different materials [26].

$$K_{de} = \frac{L_E + L_{Eb}}{\frac{L_E}{K_{dE}} + \frac{L_{Eb}}{K_{dEb}}} = \frac{B + H_b{\cdot}N_b}{\frac{H_b{\cdot}N}{K_{dE}} + \frac{B + H_b{\cdot}(N_b - N)}{K_{dEb}}} = \frac{B + H_b{\cdot}N_b}{\frac{K_{dEb}{\cdot}(H_b{\cdot}N) + K_{dE}{\cdot}(B + H_b{\cdot}(N_b - N))}{K_{dE}{\cdot}K_{dEb}}}$$
$$= \frac{K_{dE}{\cdot}K_{dEb}{\cdot}(B + H_b{\cdot}N_b)}{K_{dEb}{\cdot}(H_b{\cdot}N) + K_{dE}{\cdot}(B + H_b{\cdot}(N_b - N))} \quad (16)$$

where

K_{dE} represents the linear permeability of the material of the downstream shoulder of the dam,

K_{dEb} represents the linear permeability of the rockfill toe protection.

The average velocity at the upstream end of the seepage area (Fig. 4) can be expressed with (Eq. (17)):

$$v = \frac{q_s}{H_b} \quad (17)$$

From (Eq. (12)) and (Eq. (17)), following the above mentioned assumption about the length of the seepage paths:

$$\frac{q_s}{H_b} = K_{de}{\cdot}\frac{H_b}{L_E + L_{Eb}} \quad (18)$$

Similarly, applying the linear seepage equation to the through-flow in the case of the seepage through the material of the rockfill shoulder at the toe of the dam (Fig. 2) and considering the same assumption for the length of the seepage path:

$$\frac{q_s}{z_d} = K_{dE}{\cdot}\frac{z_d}{N{\cdot}z_d} \quad (19)$$

Matching q_s from (Eq. (18)) and (Eq. (19)):

$$K_{de}{\cdot}\frac{H_b^2}{L_E + L_{Eb}} = K_{dE}{\cdot}\frac{z_d^2}{N{\cdot}z_d} \quad (20)$$

Since

$$L_E + L_{Eb} = B + H_b{\cdot}N_b \quad (21)$$

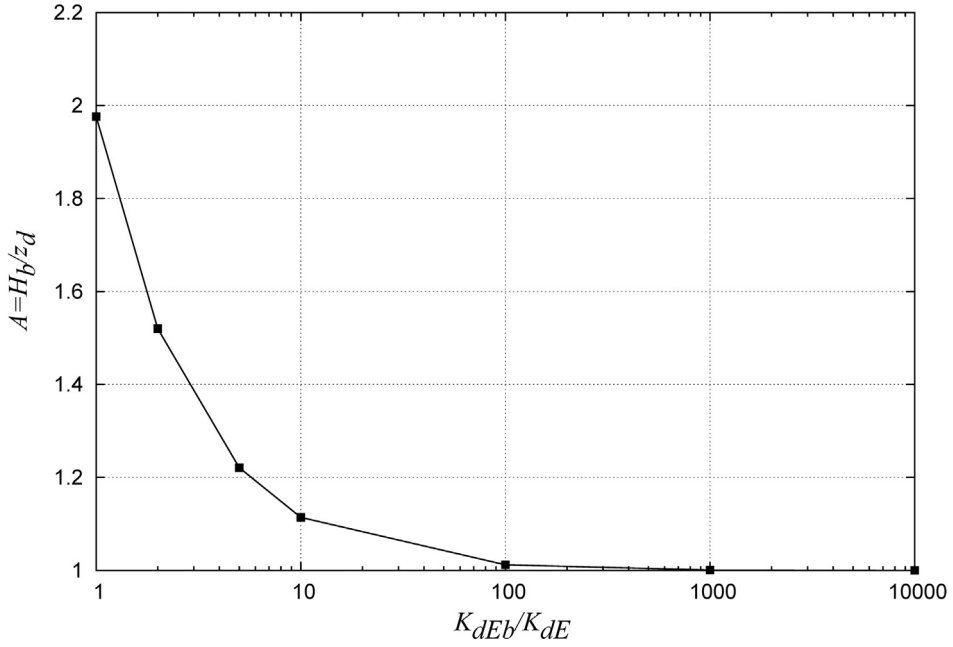

Fig. 6. Evolution of coefficient A with the permeability ratio K_{dEb}/K_{dE} [26].

it is possible to reorganize (Eq. (20)):

$$K_{de}\cdot H_b^2 = K_{dE}\cdot\frac{B + H_b\cdot N_b}{N\cdot z_d}\cdot z_d^2 \tag{22}$$

Substituting H_b in (Eq. (22)) from (Eq. (10)):

$$K_{de}\cdot A^2\cdot z_d^2 = K_{dE}\cdot\frac{B + A\cdot z_d\cdot N_b}{N\cdot z_d}\cdot z_d^2 \tag{23}$$

Reorganizing (Eq. (23)):

$$K_{de}\cdot A^2 = K_{dE}\cdot\frac{B + A\cdot z_d\cdot N_b}{N\cdot z_d} \tag{24}$$

Substituting H_b (Eq. (10)) in K_{de} (Eq. (16)) and this one in (Eq. (24)):

$$\frac{K_{dE}\cdot K_{dEb}\cdot(B + z_d\cdot N_b\cdot A)}{K_{dEb}\cdot z_d\cdot N\cdot A + K_{dE}\cdot(B + z_d\cdot(N_b - N)\cdot A)}\cdot A^2 = K_{dE}\cdot\frac{B + z_d\cdot N_b\cdot A}{N\cdot z_d} \tag{25}$$

The obtained expression (Eq. (25)) is a transcendental equation where all variables have known values except A, which is the unknown to be obtained by conventional numerical methods. Once A is evaluated, this can be used to estimate the height of the protection (H_b) using (Eq. (10)).

Applying (Eq. (25)), the effect of the relation between the equivalent permeability of the materials E and E_b on the design of the protection can be analyzed. Fig. 6 shows the evolution of the coefficient A, i.e., the height of the rockfill protection, depending on the permeability ratio between the protection and dam materials (K_{dEb}/K_{dE}).

The results show the benefit of using a high permeability ratio between materials E_b and E for the design of rockfill protection, as expected. Thus, as the ratio K_{dEb}/K_{dE} increases, the coefficient A tends to one, which is a minimum theoretical value. Furthermore, the height of the protection exponentially increases as this ratio tends to zero. Therefore, values of K_{dEb}/K_{dE} lower than 5 should be avoided in practice in order to get a cost-effective design.

3. Summary of the design procedure

In summary, the design procedure allows obtaining the parameters B, N_b and H_b, for a given unit through-flow and the features of the rockfill materials (E and E_b). Such procedure is summarized in the following flowchart (Fig. 7).

Assuming all the needed data are available, the procedure follows these steps:

i. Evaluation of the width of the rockfill toe berm (B). The research studies have shown that the width of the berm must have a certain minimum dimension to enable appropriate compaction of the rockfill layers during construction.
ii. Estimation of the slope of the rockfill toe (N_b) using (Eq. (2)).
iii. Before obtaining the height of the protection (H_b), a seepage calculation of the downstream shoulder of the existing dam for the design through-flow unit discharge (q_d) is needed. The computational seepage model will be used to find the height of the saturation line at the exit in the surface of the downstream slope of the rockfill, z_d (making q_s equal to the value q_d in Fig. 2). This numerical model must consider the parabolic seepage equation (Eq. (1)) of the material of the downstream shoulder of the existing dam (material E). With regard to this task, the authors have developed an *Open Multi-Processing* parallel computational 3-dimensional (3D) fluid dynamic code to solve the Navier–Stokes equations [20]. The tool is able to track the evolution of the free surface using a level set technique, and it can be used for the simulation of any problem involving free surface flows, such as the hydraulic analysis of dam spillways. Moreover, the formulation was conceived to be able to take into consideration the presence of a rockfill-like porous material and to simulate its internal seepage evolution [32,34]. The governing equations are discretized using a classical Galerkin approximation and simplicial elements are used. A stabilization technique is therefore required to overcome the stability issues. We use a subgrid-scale technique for this purpose. All the details of the numerical formulation can be consulted in [31]. There are additional techniques based on experimental research that can be also considered to estimate z_d [35,36].
iv. Once the value of z_d has been obtained, the protection height (H_b) can be estimated through (Eq. (10)) and (Eq. (25)).
v. The final design should be numerically modeled to check the fulfillment of the condition for the design through-flow (Eq. (6)).
vi. Additional measures to avoid internal and external erosion should be considered by adding transition layers between the dam and protection materials or sizing the riprap layer of the external surface of the rockfill protection.

4. Experimental validation

4.1. General approach

The previously described design procedure was validated experimentally through a set of blind tests to verify the stability of the dam and protection. The test model was considered as the prototype for the

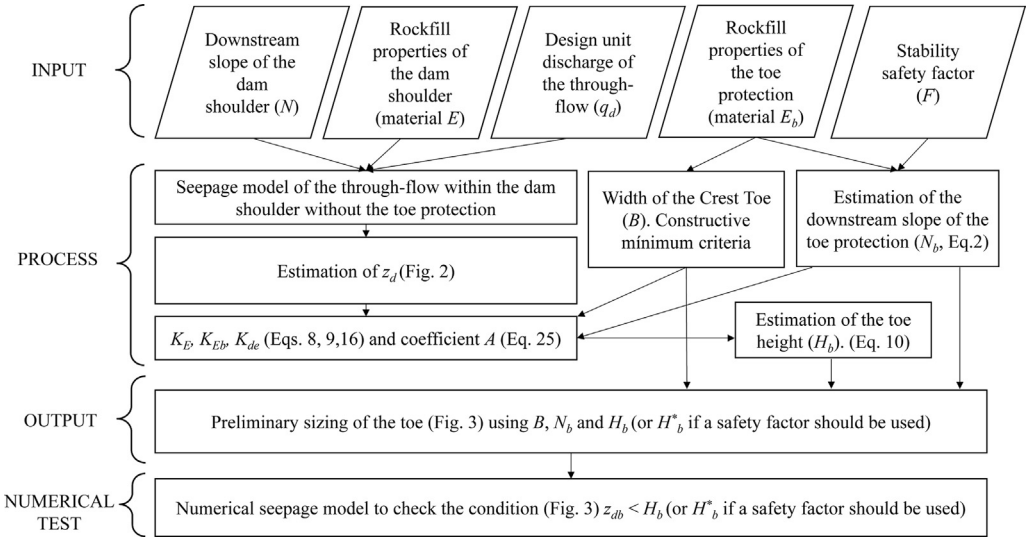

Fig. 7. Flowchart of the methodology to design rockfill toe protections.

verification. Thus, no similarity criterion was considered necessary to validate the proposed methodology. It was assumed that the same physical phenomenon is present in the test model and in any real size prototype and, accordingly, the equations governing the mass slide will be the same as well.

In such tests, two different pairs of both dam and protection materials were used. Homogeneous gravels of sizes (D_{50}) 12.6 mm (*M*1), 35.0 mm (*M*2) and 45.0 mm (*M*3) were combined to design four cases of rockfill toe protection according to the new procedure. The tests were proposed in advance such that each protection was designed following the new methodology. Once the geometric variables of each protection were obtained, they were tested in the laboratory in order to compare the results with the theoretical behavior and, accordingly, validate or refute the methodology.

Therefore, even though the damages caused by erosion or particle dragging were registered by the instrumentation devices, they were not considered in the analysis of the protection stability. To do so, the research established criteria to distinguish between the damages caused by the two predominant mechanisms of failure, either mass sliding or particle dragging [26]. This analysis became complex for unit flows near the threshold unit-flow when particle dragging initiates.

In addition to this, two failure tests of the unprotected dam were developed as reference cases in order to be able to compare the degree of protection achieved by every rockfill toe during validation. The materials used in these failure tests were *M*1 and *M*2, respectively.

4.2. Laboratory facility and description of the materials

The validation tests were performed in a 13.7 m long, 1.4 m high and 2.4 m wide channel with a horizontal bottom. The channel has three functional areas (Fig. 8). From upstream to downstream, there is a 1 m long inlet and energy dissipation area, a 9.5 m long testing area and a 3.2 m long particle catchment and sink flow area. On its right wall (in the flow direction), there is a 4.6 m long and 1.1 m high glass window for visual inspection and also for video and photographic recording during the tests. In this particular test campaign, the channel width of the facility was narrowed to 1.32 m by adding a longitudinal internal separation wall.

The test facility has an inlet pipe which can provide a maximum flow of 340 L s^{-1}. There is an electronically controlled valve to manage the inflows. All the testing flows were constant in each flow stage, making all the measurements in steady state conditions. The main instrumentation of the tests consisted of:

- Flow measurement. Flow discharge was measured by an ultrasonic flowmeter (*Fluxus ADM 7407*). Prior to the start of the tests, the measurements of the equipment were checked by the ones obtained by a discharge measurement structure consisting of a rectangular sharp-crested weir at the end of the sink flow area (Fig. 8).
- Water surface measurement. Three ultrasonic level meters were used, two of them installed in the testing area, upstream and downstream of the model (1 m and 8 m downstream of the inlet area, respectively).
- Digital modeling device (*DMD*). The *DMD* consists of a computer-controlled laser equipment (*SICK LMS200-30106*). Such equipment is able to measure radial distances in order to obtain a single profile of the model. The laser device is installed on a mobile frame in such a way that it is able to move along the transverse axis of the channel, obtaining as many profiles as needed to obtain the coordinates of the points of the external surface of the model. This operation is controlled automatically by a computer. The obtained coordinates of the points are exported to a text file. This file is then imported by the preprocessing software *GID*^{TM} to generate the mesh of the external surface of the model (Fig. 9). Once the mesh is generated, this information can also be used for different post-processing analyses such as detection of modified surfaces or comparisons between relevant cross-sections.

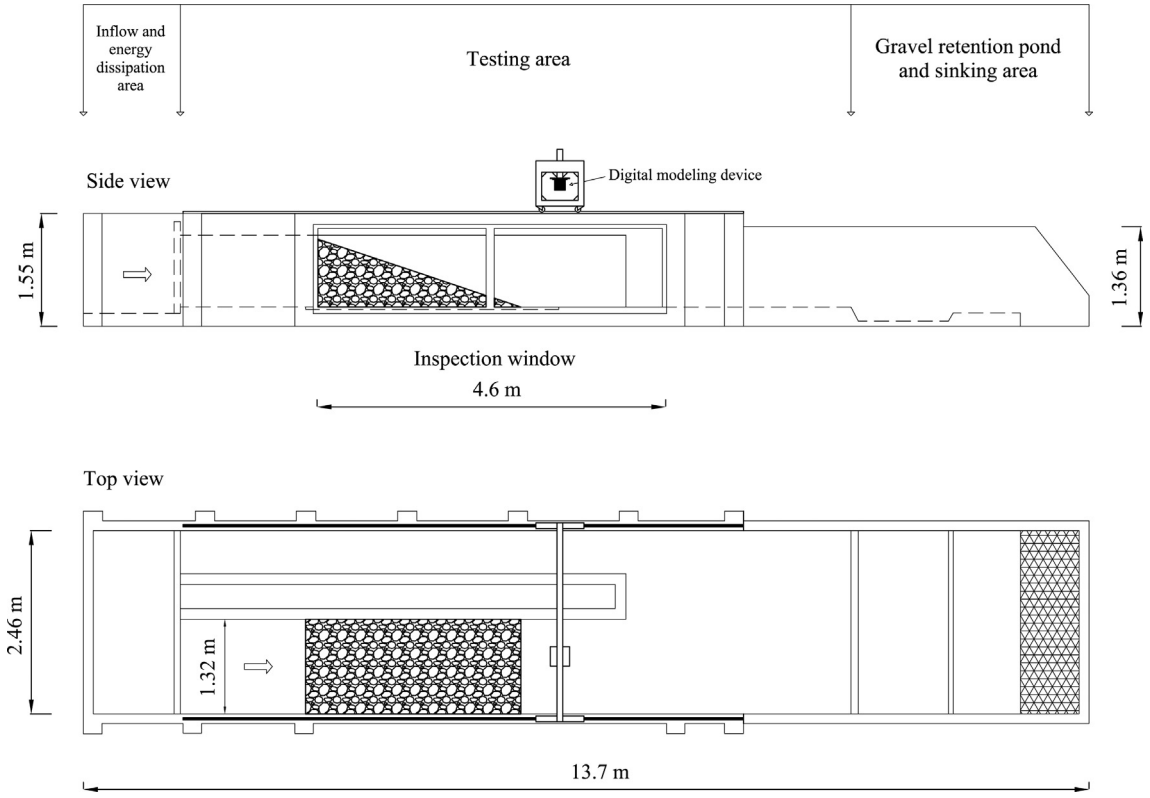

Fig. 8. Side and top view of the laboratory facility ().
adapted from [29]

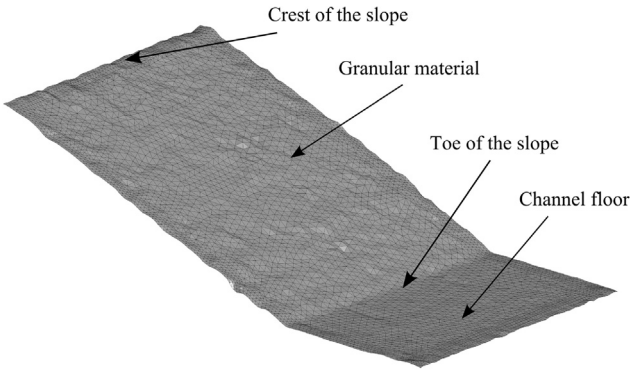

Fig. 9. Example of a generated model mesh with slope 2.6:1 (H:V) tested in the 1.32 m wide channel.

The types of granular material used in the tests were limestone gravels from the same quarry, with three different grading curves (Fig. 10). Internal friction angles were determined by measuring the angle of repose of 6 samples, composed of 0.5 m high, 1.32 m long stone fills. These fills were formed by dropping the granular material. After the fill placement in dry conditions, 100 cross-section profiles, spaced every 1 cm in the middle part of the sample, were obtained by means of the *DMD*. In this way, the angle of repose of each profile could be obtained. The friction angle adopted for each stone fill was the average of the repose angles of such profiles. Likewise, the friction angle of the material was the average of each stone fill. In such a way, a total of 600 cross-section profiles were considered in the analysis. In addition to this, material properties such as porosity (n), uniformity coefficient (C_u), particle size (D_x) and internal friction angle (φ) were also obtained (Table 1).

Also, the coefficients a and b of the parabolic seepage equation (Eq. (1)) were experimentally obtained for each material by means of specific through-flow tests in samples of gravel with a slope 3:1 (H:V). Hydraulic gradients and average seepage velocities were obtained from these tests (Fig. 11) using the measurements of pressure heads along the base of the model [26].

Table 1
Properties of the materials used in the validation tests.

Material	D_{50} (mm)	n	C_u (D_{60}/D_{10})	φ (°)	$\gamma_{e,sat}$ (kN m^{-3})
M1	12.6	0.41	1.5	36.9	19.25
M2	35.0	0.41	1.6	41.3	18.50
M3	45.5	0.41	2.3	41.7	18.98

Then, the coefficients a, b in (Eq. (1)) were obtained for the three materials using a least square minimization of the error of a parabolic function. Results are shown in Table 2:

where

RSS is the sum of squares of residuals of the regression through a second-order polynomial fit.

4.3. Description of the validation tests

The validation tests were posed to protect two different 1 m high dam shoulders with slopes designed according to the Spanish regulation for dams [38] which applies 1.4 as the mass-slide safety factor in normal operation. Note that this safety factor has been set considering the absence of pore water pressures within the downstream shoulder of the dam, as is usual in the dam engineering criteria. The materials used for the dam shoulder were *M*1 and *M*2. Such materials were placed in the facility without compaction in order to guarantee an isotropic behaviour. As has been indicated in the overview, this procedure is applicable only for isotropic materials such as “clean” rockfills with negligible segregation caused by the compaction energy of the machinery during construction, for example.

The comparison of the behavior between the dam with and without protection made necessary to make additional tests to register the damages on the unprotected dam for different through-flows. Such tests were considered as the *reference cases*. Thus, the particular unit through-flow discharges which caused the total failure of the unprotected dam shoulder (q_r) were registered, and such unit discharges were considered in the analysis of the effect of the protection. A

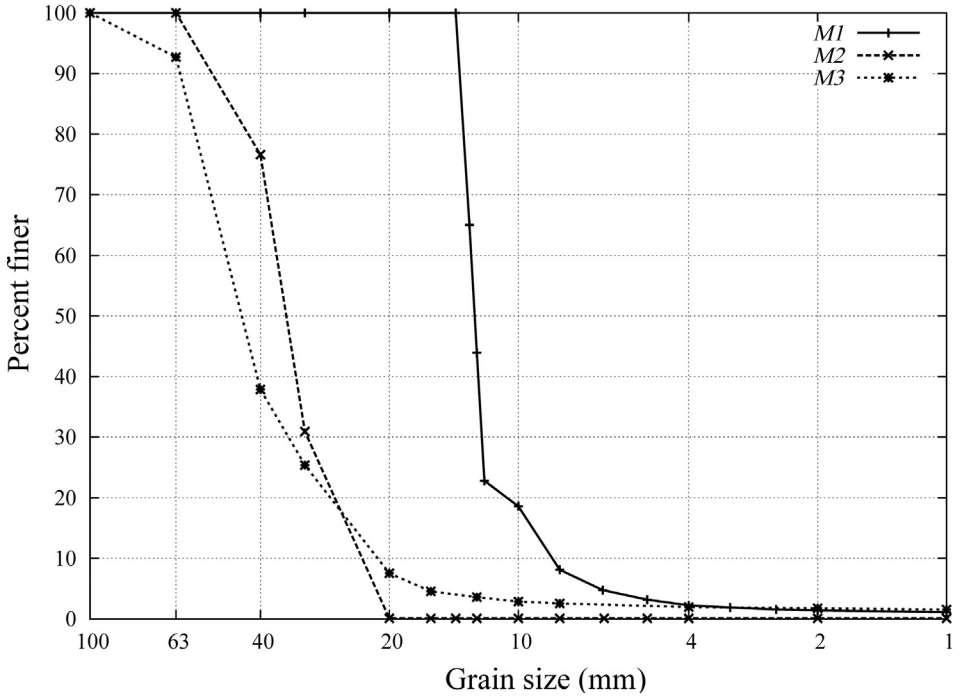

Fig. 10. Grading curves of materials used in the validation tests ().
adapted from [37,36]

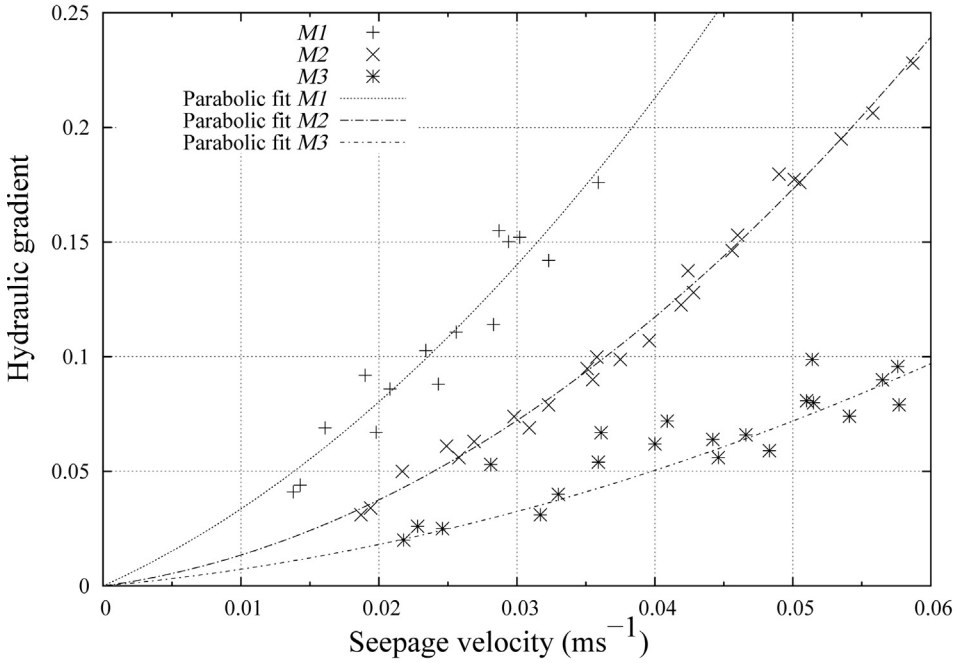

Fig. 11. Hydraulic gradients experimentally obtained for different seepage velocities and materials [36].

Table 2
Results of the experimental calibration of the parabolic seepage equation of the materials used in the validation tests.

Material	a (sm^{-1})	b (s^{2}m^{-2})	*RSS*
M1	2.71	65.35	2.2×10^{-3}
M2	0.82	52.82	6.4×10^{-4}
M3	0.65	16.96	1.8×10^{-2}

summary of the data of the validation tests is shown in Table 3. The validation tests are labelled *Mj_M(j + 1)_q_d*, where *Mj* is the dam material and *M(j + 1)* is the material of the protection, q_d is the design unit discharge (in Ls^{-1} m^{-1}) and j = 1,2.

Consequently, considering the data of each validation test (Table 3), the corresponding rockfill toe protections were defined by applying the proposed design methodology (Table 4). In these cases, the criterion to establish the width of the berm (B) was to be four times the size D_{50} of the protection material. In tests *12_35_10* and *12_35_16*, the heights of the protections used for the experimental validation (H_b^*) were the same as those obtained from the procedure (H_b), i.e., the safety factor was 1 for the variable H_b. The tests *35_45_35* and *35_45_45* were performed with a safety factor of 1.1 in order to check the performance of the protection in a more conservative scenario.

Next, the toe protections were prepared at the lab and tested for different through-flow discharges to verify the methodology. The effect of the protection was evaluated through the *maximum advance of the damage* (B_c), measured from the position of the downstream toe of the rockfill at the beginning of the test, in the longitudinal direction of the channel. For the unprotected dam, B_c was measured similarly, from the toe of the downstream shoulder of the dam without protection. This length can be expressed with the dimensionless ratio B_c/L, with L being the horizontal distance between the toe and the downstream end of the crest of the dam shoulder (Fig. 12). Accordingly, L_P is the horizontal distance between the downstream toe and the point P, which is the intersection between the berm crest and the slope of the dam shoulder. Thus, when B_c exceeds L_P, the dam begins to be damaged by the through-flow. The protection is considered successful if the dam is not harmed for the design unit discharge (q_d), i.e., when B_c is lower than L_P with such discharge.

As an example of how the proposed methodology was applied, the design of the rockfill toe protection of *Test 12_35_16* was as follows (according to the flowchart in Fig. 7):

1. Input data.
   a. Downstream slope of the shoulder of the existing dam: N = 1.9.
   b. Rockfill properties of the material of the downstream shoulder of

Table 3
Main data of the validation tests.

	Test *12_35_10*	Test *12_35_16*	Test *35_45_25*	Test *35_45_35*
Dam material, E (D_{50} in mm)	*M1* (12.6)	*M1* (12.6)	*M2* (35.0)	*M2* (35.0)
Protection material, E_b (D_{50} in mm)	*M2* (35.0)	*M2* (35.0)	*M3* (45.5)	*M3* (45.5)
Dam height, H (cm)	100	100	100	100
Dam slope, N (H:V)	1.9	1.9	1.6	1.6
Design unit discharge of the protection, q_d (m^2 s^{-1})	0.010	0.016	0.025	0.035
Unit discharge causing the failure of the unprotected dam, q_r (m^2 s^{-1})	0.020	0.020	0.034	0.034
q_d/q_r ratio	0.50	0.80	0.73	1.02
K_{dE} (ms^{-1})	0.14	0.14	0.16	0.16
K_{dEb} (ms^{-1})	0.21	0.21	0.36	0.36
K_{de} (ms^{-1})	0.16	0.16	0.22	0.22
z_d (m)	0.18	0.27	0.29	0.37
A	1.51	1.45	1.46	1.44
H_b (m)	0.28	0.40	0.42	0.53

Table 4
Dimensions of the rockfill toe protections corresponding to the validation tests.

	Test *12_35_10*	Test *12_35_16*	Test *35_45_25*	Test *35_45_35*
Berm width, B (cm)	14	14	18	18
Rockfill toe slope N_b (H:V)	2.9	2.9	2.8	2.8
Safety factor applied to H_b (Table 3)	1	1	1.1	1.1
Rockfill toe height, H_b^* (m)	0.28	0.40	0.47	0.59
L_P/L	0.41	0.53	0.64	0.74

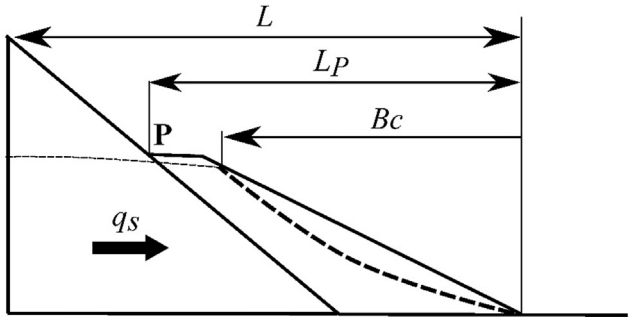

Fig. 12. Definition scheme of the maximum advance of the breakage (B_c) (). adapted from [5]

the existing dam: $a_E = 2.71$ sm^{-1}, $b_E = 65.35$ s^{-2} m^{-2}, $\varphi_E = 36.9°$ and $\gamma_{E,sat} = 19.25$ kN m^{-3}.

c. Overtopping design unit discharge: $q_d = 0.016$ m^2 s^{-1}.

d. Rockfill properties of the material of the toe protection: $a_{Eb} = 0.82$ s m^{-1}, $b_{Eb} = 52.82$ s^{-2} m^{-2}, $\varphi_{Eb} = 42.0°$ and $\gamma_{Eb,sat} = 18.85$ kN m^{-3}.

e. Required stability factor in overtopping for validation: $F = 1$.

2. Process.

a. Seepage model of the existing dam without any protection (using Kratos). As a result of that, $z_d = 0.273$ m is obtained.

b. Width of the crest toe according to a constructive minimum: $B = 4D_{50} = 0.14$ m, where D_{50} is referred to the material of the protection. In this case, it was considered reasonable to follow the criteria of using the average size of the stones (35 mm) multiplied by four.

c. Calculation of the downstream slope of the toe protection (Eq. (2)) considering $\beta = 1$, specific weight of the water $\gamma_w = 10$ kN m^{-3}, $\varphi_{Eb} = 41.3°$; $\gamma_{Eb,sat} = 18.5$ kN m^{-3}. The corresponding slope is $N_b = 2.88$ (angle $\alpha = 19.1°$). As the value of N_b is greater than 2, the hypothesis of considering $\beta = 1$ is correct. The slope of the protection was approximated to 2.9 (H:V) for the following steps.

d. Applying (Eq. (8)) and (Eq. (9)), the values of K_{dE} and K_{dEb} are 0.14 ms^{-1} and 0.21 ms^{-1}, respectively, i.e., $K_E = 7.37$ sm^{-1} and $K_{Eb} = 4.70$ sm^{-1}.

e. Finally, solving (Eq. (25)) for the unknown variable A the obtained value for this factor is 1.45. Thus, according to (Eq. (10)) the height of the toe (H_b) is 0.397 m. Rounding to the second decimal, the proposed height was 0.40 m.

3. Output. In summary, as a result of the procedure explained above, the proposed sizing for the rockfill toe was a width of the toe berm (B) of 14 cm, a downstream slope (N_b) of 2.9 (H:V) and a height of the berm (H_b) of 40 cm. The safety factor for this variable for both the tests *12_35_10* and *12_35_16* was 1. Hence, the height of the toe for the experimental validation (H_b^*) was 40 cm (the same as H_b).

4. Final test. A numerical seepage model was done with the proposed protection to verify the required condition $z_{db} < H_b$. The value of z_{db} resulting from the numerical model was 37.8, which fulfilled the requirement, and the protection was proposed for experimental validation at the lab.

4.4. Results of the validation tests

The results of the tests are shown in Fig. 13. Each data series represents the *failure paths* [26] of both the unprotected and protected dam shoulder. Such failure path shows the evolution of the dimensionless maximum advance of the damage (B_c/L) for different unit through-flow discharges (q_s) registered at each test. In the abscissa, such unit through-flow discharge is represented as a dimensionless parameter referring to the unit flow which causes the total failure of the unprotected dam (q_r). The results of B_c were measured independently of the prevailing mechanism of failure. In this regard, during the validation tests, it was observed that the predominant failure mechanism for unit discharges higher than q_d was particle dragging of the stones located at the external surface of the sample. Fig. 13(a) shows the evolution of the failure of the protections *12_35_10* and *12_35_16* for the design unit discharge of 50% (0.010 m^{2}s^{-1}) and 80% (0.016 m^{2}s^{-1}) of the unit discharge which caused the failure of the unprotected dam, respectively. Similarly, Fig. 13(b) shows the evolution of the failure of the protections *35_45_25* and *35_45_35* for the design unit discharge of 73% (0.025 m^{2}s^{-1}) and 102% (0.035 m^{2}s^{-1}) of the failure unit discharge of the unprotected dam, respectively. Note that, in Fig. 13, the rockfill protection extends from the toe (0 in the axis B_c/L) to the point P (L_P/L in the same axis) for each validation case. Therefore, the damages affect the material of the protected dam since the moment that failure path surpasses such point.

4.5. Discussion of the validation

The results of the tests showed that protection increased the stability of the dam. In particular, for the design unit discharge (see example in Fig. 14) the dam was not harmed, as expected. Furthermore, the damages observed for higher unit discharges were caused mainly by dragging of particles, and the conclusions of the tests indicated that the effect of the protection remained even for unit discharges higher than the design value.

The failure paths (Fig. 13) show the achieved degree of protection through the difference of the maximum breakage (B_c/L) of both the unprotected (reference case) and protected dam. The protection effect continued even for through-flows higher than q_d. Thus, in the *12_35* tests (Fig. 13(a)), the dimensionless design unit through-flows (q_d/q_r) were 0.5 and 0.8. However, for a value of 0.9, higher than the design values in both cases, the performance of the protection was even better as expected, as can be checked in Fig. 13, through the difference of the B_c/L values and the ones corresponding to the case of the unprotected dam. Thereby, the damages on the protected dam were limited to values between 20% and 30% while the unprotected dam was harmed approximately on 85% of its height. This fact was more pronounced in the *35_45* tests, where the protected dam increased the value of the unit discharge which produced the total failure (B_c/L equal to one), between 50% and 70% regarding the unit discharge which made the unprotected dam fail, i.e., q_d/q_r equal to 1. This improvement of the performance of the protection even for unit discharges higher than q_d implies an additional benefit of this kind of protection. Regarding this, it has to be noted that in the *35_45* tests a factor of safety of 1.1 was considered to increase the height of the toe at the experiments (H_b^*) from the value of the height obtained through the procedure (H_b). Thus, a higher

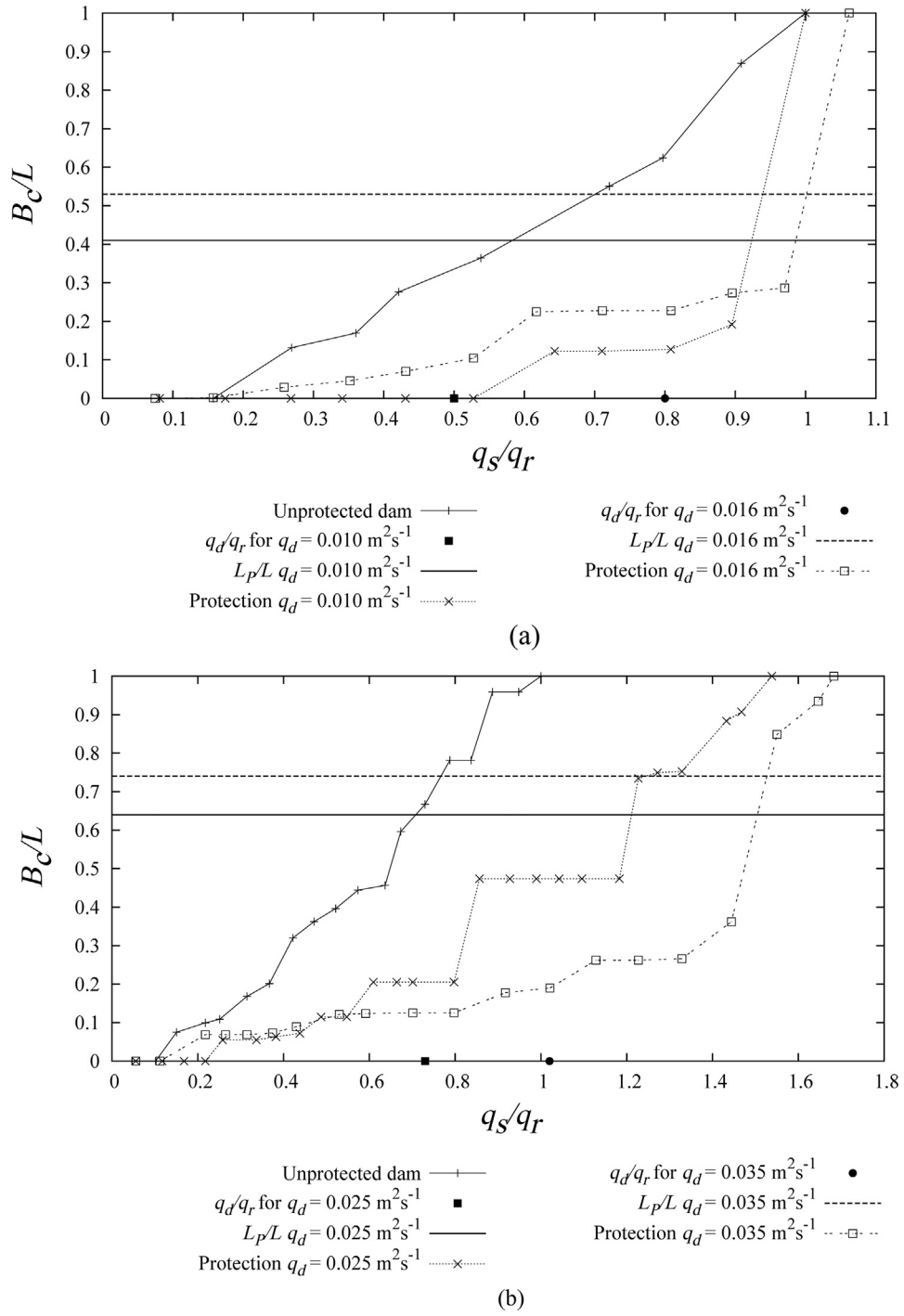

Fig. 13. Failure paths obtained from of the validation tests. (a) Tests *12_35_10* and *12_35_16*. (b) Tests *35_45_25* and *35_45_35* (). adapted from [5,26]

resistance might be expected. In conclusion, the results obtained in the four experimental tests validated the proposed methodology.

Additionally, it was concluded that the performance of the protection may be increased by a specific treatment of the external area of the downstream slope of the rockfill in order to avoid the dragging of stones at the outer surface. This can be done through a rockfill layer with specific sizing to avoid particle dragging for specific unit discharge [16,39,40] or other techniques such as reinforced rockfill or reinforced fill [7]. It seems this complement could increase the degree of protection significantly, as was noted on the tests where the effect of the dragging of particles was reduced.

5. Summary and conclusions

A new design methodology for rockfill toe protections to ensure the mass-slide stability of dams with a highly permeable downstream shoulder during accidental through-flow processes has been presented. Such processes can be caused by overtopping or extreme internal leakage, which are the main causes of embankment dam failures. The procedure may be applicable when the rockfill materials of the downstream shoulder and the protection are both highly isotropic. Such procedure uses as inputs the overtopping unit discharge, the slope of the downstream shoulder of the existing dam and the geotechnical

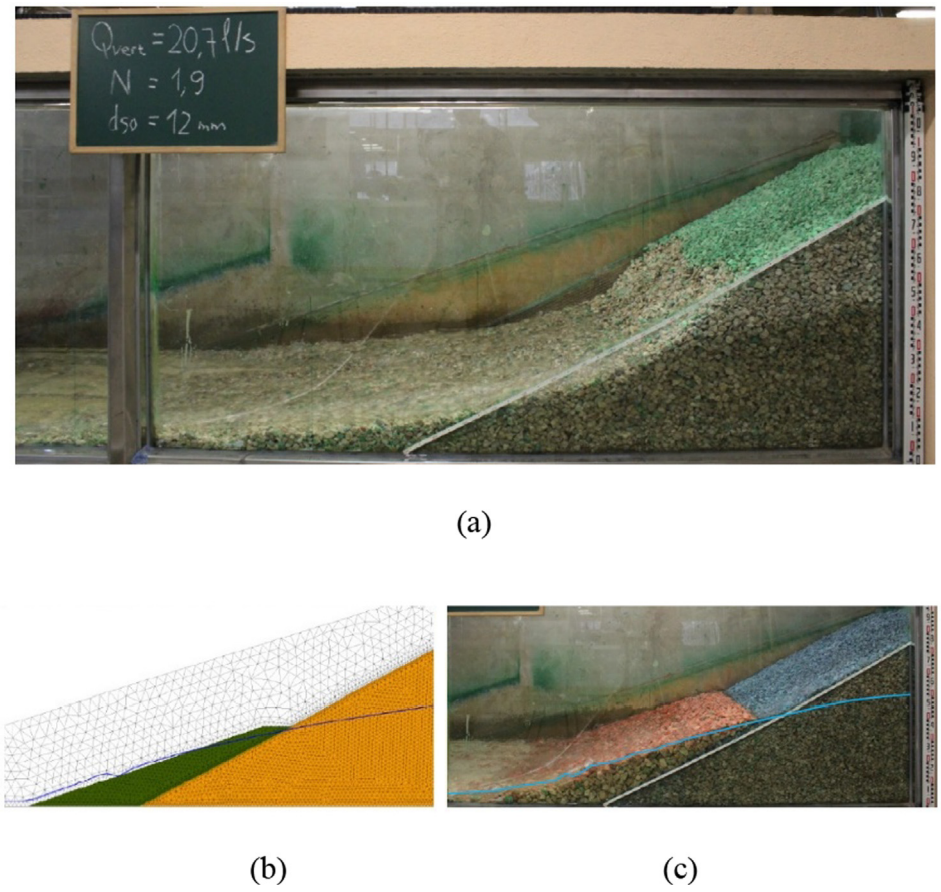

Fig. 14. Test *12_35_16*. (a) Photo showing the damage in the dam without any protection for q_d. (b) Numerical model of the same through-flow with the proposed protection. (c) Photo of the corresponding validation test. [5,26].

characterization of the rockfill of both the existing dam and toe protection. The process involves turbulent seepage numerical modelling and the application of a simplified methodology to help the dam engineer to propose the design of the toe. The output of the procedure is the geometry of the toe protection for a given mass-slide safety factor.

Even though this methodology has been experimentally validated for the stabilization of the downstream shoulder, there are additional issues to be considered in a project of this kind of protection, for example, problems such as the potential scour of the foundation, the undermining of the dam (or toe) rockfills, and the particle dragging of the stones located at the external surface of the toe slope due to the macroturbulent actions of the flow on the shoulder. For such reasons, future research lines to improve the overall performance of this kind of protection should be focused on studying external reinforcements against particle dragging caused by the outflow at the toe and the likelihood of internal erosion of rockfills in turbulent through-flow scenarios.

Acknowledgements

This research was developed with funds from the Spanish National Research and Development Program (2008–2011) of the Spanish Ministry of Science and Innovation through the research project titled "*Rotura del elemento impermeable de presas de materiales sueltos en situación de sobrevertido y análisis de protecciones combinando modelación física e inteligencia artificial*", with ID code *BIA2010-21350-C03-03*. The authors also gratefully acknowledge the help of Prof. Eugenio Oñate, Dr. Fernando Salazar, and Prof. Riccardo Rossi.

References

[1] Kompetanse EBL. Stability and breaching of embankment dams. Report on Subproject 2: Stability of downstream shell and dam toe during large through-flow. Oslo (Norway): EBL Kompetanse AS; 2005.
[2] Swedenergy. Kraftföretagens riktlinjer för dammsäkerhet. RIDAS (Swedish Hydropower companies guidelines for dam safety, application guideline), Stockholm (Sweden): Svensk Energi; 2007 [In Swedish].
[3] Lempérière F. Overspill rockfill dams: Conventional and unconventional designs. Technology-costs-safety. Proceedings of ICOLD Viena Congress, Austria 1991;Q67:111-27.
[4] FEMA. Technical Manual: Overtopping Protection for Dams: U.S. Department of Homeland Security; 2014.
[5] Morán R. Review of embankment dam protections and a design methodology for downstream rockfill toes. In: Toledo MÁ, Morán R, Oñate E, editors. Dam protections against overtopping and accidental leakage: CRC Press; 2015. p. 25–40.
[6] ICOLD. Bulletin 99. Dam Failures Statistical Analysis. Paris (France): International Committee on Large Dams; 1995.
[7] ICOLD. Bulletin 89. Reinforced rockfill and reinforced fill for dams- State of the art-, Paris (France): International Committee on Large Dams; 1993.
[8] Charman J, Kostov L, Minetti L, Stoutesdijk J, Tricoli D. Small dams and weirs in earth and gabion materials. Rome (Italy): Food and Agriculture Organization of the United Nations (FAO); 2001.
[9] Fratino U, Renna FM. Flow features on gabion stepped weirs. 33rd IAHR Congress: Water Eng Sustain Environ 2009:2319–26.
[10] Chinnarasri C, Donjadee S, Israngkura U. Hydraulic characteristics of gabion-stepped weirs. J Hydraul Eng 2008;134:1147.
[11] Frizell KH, Ruff JF, Mishra S. Simplified design guidelines for riprap subjected to overtopping flow. Proceedings of the Annual Conference of the Assoc of State Dam Safety Officials 1998:301–12.
[12] Ministry of Petroleum and Energy. Regulations governing the safety and supervision of watercourse structures. Oslo (Norway): Energy Water Resources Department; 2000.
[13] Nilsson A, Norstedt U. Commentary on the chapter of embankment dams in the Swedish Dam Safety Guidelines. Dam Safety: Proceedings of the International Symposium on New Trends and Guidelines on Dam Safety, Barcelona, Spain; 1998. p. 23–9.
[14] Bartsch M, Nilsson Å. Leakage in embankment dams. Functional analysis and strengthening by adding a downstream berm. In: Proceedings of Talsperren

Symposium Deutschen TalsperrenKomitee Freising, Germany; 2007. p. 15–20.
[15] Nilsson A. Maximal credible leakage for large rockfill dams due to internal erosion. International Workshop on Internal Erosion in Dams and Foundations Saint Petersburg, Russia; 2009.
[16] Lia L, Vartdal E, Skoglund M, Campos H. Rip rap protection of downstream slopes of rock fill dams-A measure to increase safety in an unpredictable future climate. In: Proceedings of the 9th ICOLD European Club Symposium, Venice, Italy; 2013.
[17] Toledo MA. Embankment dams slip failure due to overtopping. Trans Int Congr Large Dams 1997;4:317–30.
[18] Toledo MA, Morán R, Campos H. Modelación del movimiento del agua en medios porosos no lineales mediante un esquema de diferencias finitas. Aplicación al sobrevertido en presas de escollera. Revista Internacional de Métodos Numéricos para Cálculo y Diseño en Ingeniería 2012;28:225–36.
[19] Fry JJ, Beguin R, Picault C, Mathieu F, Esnault A, Mosser J. Analysis and treatment of internal erosion: conventional and new methods. Proceedings of ICOLD Stavanger Congress, Norway 2015;Q98:604–25.
[20] Rossi R, Larese A, Dadvand P, Oñate E. An efficient edge-based level set finite element method for free surface flow problems. Int J Numer Methods Fluids 2012;71:687–716.
[21] Larese A, Rossi R, Oñate E. Coupling eulerian and lagrangian models to simulate seepage and evolution of failure in prototype rockfill dams. In: Proceedings of XI ICOLD Benchmark Workshop on Numerical Analysis of Dams, Valencia, Spain; 2011. p. 1–20.
[22] Larese A, Rossi R, Oñate E. In: Toledo MA, Morán R, Oñate E, editors. Dam protections against overtopping and accidental leakage. Great Britain: CRC Press; 2015. p. 111–21.
[23] Toledo MA. Diseño de presas de escollera resistentes al sobrevertido [In Spanish]. Madrid, Spain: Comité Nacional Español de Grandes Presas; 1998.
[24] Toledo MA, Morera L. Design of overtopping-resistant rockfill dams. In: Toledo MA, Morán R, Oñate E, editors. Dam protections against overtopping and accidental leakage. Great Britain: CRC Press; 2015. p. 133–42.
[25] Toledo MA, Morera L. Isoresistant double slope for the optimization of overtopping-resistant rockfill dams. In: Toledo MA, Morán R, Oñate E, editors. Dam protections against overtopping and accidental leakage. Great Britain: CRC Press; 2015. p. 143–50.
[26] Morán R. Improvement of the safety of rockfill dams during through-flow processes using downstream rockfill toes [In Spanish]. Ph D Thesis Universidad Politécnica de Madrid; 2013. p. 1–384.
[27] Parkin AK. Field solutions for turbulent seepage flow. J Soil Mech Found Div 1971;97:209–18.
[28] Lawson JD, Trollope DH, Parkin AK. In: Silvester R, editor. Hydraulics and fluid mechanics. Proceedings of the First Australasian Conference: Pergamon Press; 1962. p. 159–172.
[29] Morán R, Toledo MA. Research into protection of rockfill dams from overtopping using rockfill downstream toes. Can J Civ Eng 2011;38:1314–26.
[30] Dadvand P, Rossi R, Oñate E. An object-oriented environment for developing finite element codes for multi-disciplinary applications. Arch Comput Methods Eng 2010;17:253–97.
[31] Larese A, Rossi R, Oñate E, Idelsohn S. A coupled PFEM–Eulerian approach for the solution of porous FSI problems. Comput Mech 2012;50:805–19.
[32] Larese A, Rossi R, Oñate E. Finite element modeling of free surface flow in variable porosity media. Arch Comput Methods Eng 2015;22:637–53.
[33] Gonzalez de Vallejo L, Ferrer M, Ortuño L, Oteo C. Ingeniería Geológica. Madrid, Spain: Pearson Educación; 2002.
[34] Larese A, Rossi R, Oñate E, Toledo MÁ, Morán R, Campos H. Numerical and experimental study of overtopping and failure of rockfill dams. Int J Geomech 2015;15:04014060.
[35] Hansen D, Zhao W, Han S. Hydraulic performance and stability of coarse rockfill deposits. In: Proceedings of the Institution of Civil Engineers-Water Management Thomas Telford Ltd 2005;158:163–75.
[36] Monteiro-Alves R, Toledo MÁ, Morán R. Characterization of the overtopping flow through the downstream shell of rockfill dams. J Hydraul Eng 2019;145:04019015.
[37] Alves RM, Toledo MÁ, Morán R. Overflow for the complete failure of the downstream shell of a rockfill dam. In: Proceedings of Protections 2016: 2nd International Seminar on Dam Protection Against Overtopping Colorado State University Libraries; 2016.
[38] SPANCOLD. Criterios para proyectos de presas y sus obras anejas. Tomo II. Presas de materiales sueltos. [In Spanish], Madrid, Spain: Colegio de Ingenieros de Caminos, Canales y Puertos y Comité Nacional Español de Grandes Presas; 2015.
[39] Hiller PH. Riprap design on the downstream slopes of rockfill dams. Ph D Thesis. Norwegian University of Science and Technology; 2017.
[40] Abt SR, Thornton CI, Scholl BA, Bender TR. Evaluation of overtopping riprap design relationships. JAWRA J Am Water Resour Assoc 2013;49:923–37.